PNAS RESEARCH ARTICLE | PHARMACOLOGY OPEN ACCESS

A specific JMJD6 inhibitor potently suppresses multiple types of cancers both in vitro and in vivo

Rong-quan Xiao[a,b,1], Ting Ran[a,b,c,1], Qi-xuan Huang[a,b], Guo-sheng Hu[a,b], Da-meng Fan[a,b], Jia Yi[a,b], and Wen Liu[a,b,2]

Edited by Michael Rosenfeld, University of California San Diego, La Jolla, CA; received January 15, 2022; accepted July 21, 2022

Jumonji C-domain-containing protein 6 (JMJD6), an iron (Fe^{2+}) and α-ketoglutarate (α-KG)-dependent oxygenase, is expressed at high levels, correlated with poor prognosis, and considered as a therapeutic target in multiple cancer types. However, specific JMJD6 inhibitors that are potent in suppressing tumorigenesis have not been reported so far. We herein report that iJMJD6, a specific small-molecule inhibitor of JMJD6 with favorable physiochemical properties, inhibits the enzymatic activity of JMJD6 protein both in vitro and in cultured cells. iJMJD6 is effective in suppressing cell proliferation, migration, and invasion in multiple types of cancer cells in a JMJD6-dependent manner, while it exhibits minimal toxicity in normal cells. Mechanistically, iJMJD6 represses the expression of oncogenes, including Myc and CCND1, in accordance with JMJD6 function in promoting the transcription of these genes. iJMJD6 exhibits suitable pharmacokinetic properties and suppresses tumor growth in multiple cancer cell line– and patient-derived xenograft models safely. Furthermore, combination therapy with iJMJD6 and BET protein inhibitor (BETi) JQ1 or estrogen receptor antagonist fulvestrant exhibits synergistic effects in suppressing tumor growth. Taken together, we demonstrate that inhibition of JMJD6 enzymatic activity by using iJMJD6 is effective in suppressing oncogene expression and cancer development, providing a therapeutic avenue for treating cancers that are dependent on JMJD6 in the clinic.

JmjC domain-containing protein | histone demethylase | small-molecule inhibitor | anticancer activity

Significance

JMJD6 is overexpressed in multiple types of cancers and promotes tumorigenesis. The enzymatic activity of JMJD6 is often tightly linked to its cellular functions. Thus, development of effective inhibitors specifically targeting JMJD6 enzymatic activity is of great interest to treat cancers. Our results demonstrate that iJMJD6 is a specific small-molecule inhibitor targeting the enzymatic activity of JMJD6, and is potent in suppressing oncogene expression and cancer development. iJMJD6 therefore might serve as a great tool for further exploring JMJD6's function in both physiological and pathological processes and provide a promising therapeutic approach for treating JMJD6-driven cancers.

Protein methylation is one of the most frequently occurring posttranslational modifications (PTMs) in mammalian cells (1). Protein methylation mainly occurs on the side chains of lysine and arginine. Protein methylation has been shown to play critical roles in a plethora of cellular processes (2). Similar to other PTMs, methylation is reversible and dynamically regulated by protein methyltransferases and demethylases. Two classes of protein demethylases have been reported so far, the KDM1 and Jumonji C (JmjC) domain–containing protein family. Both families of demethylases operate via methyl-group oxidizing mechanisms, resulting in the release of formaldehyde. The KDM1 protein demethylases are FAD-dependent amine oxidases. The JmjC-domain-containing demethylases are iron (Fe^{2+}) and α-ketoglutarate (α-KG)-dependent oxidases, which are divided into seven subfamilies based on their sequence homology and substrate specificity (3). They contain a highly conserved catalytic center, consisting of a metal chelating site, α-KG salt bridge, and hydrogen interactions. However, they differ in active sites, substrate binding region, and other functional domains.

Due to the poorly understood functions of demethylases, the development of demethylase inhibitors was relatively slower compared to other epigenetic-modifying enzymes, such as methyltransferases, acetyltransferases, and deacetylases (4). Inhibitors targeting JmjC domain–containing demethylase mainly work through competing with α-KG or iron for binding, such as the broad spectrum α-KG mimic inhibitors (5) and metal chelating inhibitor (6). Combining iron-chelating and α-KG mimic motifs with fragments that extend into the substrate binding pocket is a better choice to improve the potency and selectivity. For instance, the side chains of GSK-J1, a nanomole-scale inhibitor of the KDM6 subfamily, causes a shift of the metal cation and mimics α-KG and substrate binding (7). However, it still represents a big challenge to develop highly potent and specific inhibitors for specific member in the family of JmjC domain–containing demethylases.

JMJD6 was first recognized as a phosphatidylserine receptor (PSR) localized on the plasma membrane of phagocytic cells (8). However, it was later found to localize in the nucleus of cells, functioning as an iron- and α-KG–dependent dioxygenase. It has been reported that JMJD6 is capable of removing methylation on histone and nonhistone proteins as well as noncoding RNA (9–17). JMJD6 is overexpressed in multiple types of cancers (18). Highly expressed JMJD6 protein is often associated with aggressive and metastatic behaviors of cancer cells as well as poor prognosis in cancer patients. JMJD6 regulates a plethora of biological processes to exert its critical roles in cancer

Author affiliations: [a]State Key Laboratory of Cellular Stress Biology, School of Pharmaceutical Sciences, Xiamen University, Xiamen, 361102, China; [b]Fujian Provincial Key Laboratory of Innovative Drug Target Research, School of Pharmaceutical Sciences, Xiamen University, Xiamen, 361102, China; and [c]Department of basic research and interational cooperation, Bioland Laboratory (Guangzhou Regenerative Medicine and Health Guangdong Laboratory), Guangzhou, 510530, China

Author contributions: R.-q.X. and W.L. designed research; R.-q.X., Q.-x.H., and D.-m.F. performed research; J.Y. contributed new reagents/analytic tools; R.-q.X. and W.L. analyzed data; R.-q.X. and W.L. wrote the paper; T.R. performed the molecular docking analyses; and G.-s.H. performed the bioinformatics analyses.

The authors declare no competing interest.

This article is a PNAS Direct Submission.

[1]R.-q.X. and T.R. contributed equally to this work.

[2]To whom correspondence may be addressed. Email: w2liu@xmu.edu.cn.

This article contains supporting information online at http://www.pnas.org/lookup/suppl/doi:10.1073/pnas.2200753119/-/DCSupplemental.

Published August 15, 2022.

development, including gene transcription (17, 19), splicing (20), cell proliferation (21), cell migration (21), cell invasion (22), apoptosis (23), self-renewal capacity (24), and drug resistance (25). The enzymatic activity of JMJD6 is often tightly linked to its cellular functions. Therefore, development of small-molecule inhibitors of JMJD6 is urgently needed, which will serve as a promising way to treat cancers that are dependent on JMJD6. Meanwhile, these inhibitors will help us to better understand JMJD6 cellular functions.

In this study, we characterized a small-molecule inhibitor called iJMJD6, finding that it specifically binds to the proposed α-KG and substrate binding region in the JmjC domain and potently inhibits JMJD6 enzymatic activity in cultured cells. In line with JMJD6's critical role in gene transcriptional regulation and cancer development, iJMJD6 represses the expression of oncogenes, including Myc and CCND1, and inhibits the growth of several types of cancer cells in a JMJD6-dependent manner. iJMJD6 shows favorable pharmacokinetic properties and high efficacy in cell line– and patient-derived xenograft (PDX) models of multiple types of cancers. Furthermore, iJMJD6 synergizes with other inhibitors, including JQ1 and ER degrader fulvestrant (ICI), to inhibit tumor growth.

Results

iJMJD6 Specifically Binds to JMJD6 and Competes with α-KG and the Substrate for Binding. Through structure-based virtual screening, we reported previously that a compound named WL12 is capable of inhibiting the demethylase activity of JMJD6 with a half-maximum inhibitory concentration (IC_{50}) of 149.6 ± 34.1 nM, and it binds to JMJD6 with a K_d value of 3.31 μM base on a Biacore assay (26). We renamed this compound iJMJD6 (inhibitor of JMJD6) (Fig. 1*A*). To further characterize the iJMJD6 binding specificity with JMJD6 protein, we first synthesized iJMJD6 following the two-step procedure as described (*SI Appendix*, Fig. S1*A*). The absorption and emission spectrum of iJMJD6 are shown (*SI Appendix*, Fig. S1*B*). The structure and purity of iJMJD6 was validated by using liquid chromatography-mass spectrometry (LC-MS), ^{13}C-NMR, and ^{1}H-NMR (*SI Appendix*, Fig. S1 *C–E*). The K_d value of iJMJD6 binding with JMJD6 measured by isothermal titration calorimetry (ITC) was 3.83 μM (Fig. 1*B*). In addition, thermal shift assay (TSA) and differential scanning calorimetry (DSC) results also demonstrated that JMJD6 had a higher thermal stability (T_m) in the presence of iJMJD6, supporting the binding between iJMJD6 and JMJD6 protein (Fig. 1*C* and *SI Appendix*, Fig. S1*F*). iJMJD6 binding with JMJD6 appeared to be specific as the thermal stability of the JmjC domains from a panel of demethylases did not change significantly in the presence of iJMJD6 (Fig. 1*D*).

We next characterized the binding mode between iJMJD6 and JMJD6 protein (PDB ID: 3ldb) (27). Computer modeling results revealed that, distinct from α-KG, the aromatic rings of iJMJD6 form pi–pi (π–π) stacking interactions with two aromatic residues, tryptophan 174 (Trp174) and Trp206, in JMJD6 (Fig. 1*E*). Replacement of Trp174 and Trp206 with alanine (W174A and W206A) disrupted the pi–pi interactions (*SI Appendix*, Fig. S1 *G* and *H*). The interaction surface generated by the aromatic residues was shrunk upon mutation, which reduces the binding affinity of iJMJD6 with JMJD6 protein (*SI Appendix*, Fig. S1 *G* and *H*). We also tested the role of histidine 187 (His187), a critical residue for binding to iron, in interaction with iJMJD6. Computer modeling results showed that iJMJD6 adopted almost the same binding conformation with wild-type (WT) JMJD6 protein as JMJD6 (H187A) mutant (*SI Appendix*, Fig. S1*I*). The interactions between iJMJD6 and Fe^{2+} or aromatic residues Trp174 and Trp206 were maintained (*SI Appendix*, Fig. S1*I*). Molecular dynamic simulation results showed that W174A, W206A, and H187A mutations did not significantly influence iJMJD6 interaction with Fe^{2+} (*SI Appendix*, Fig. S1 *J–L*). To support the proposed binding mode from computer modeling, both W174A and W206A mutations impaired the thermal stability of JMJD6 protein in the presence of iJMJD6, while the H187A mutation had no significant impact (Fig. 1*F*). These results highlight the requirement of Trp206 and Trp174 for the stable interaction with iJMJD6, while Fe^{2+} plays a minimal role.

Trp206 is critical for α-KG binding, and Trp174 is close to the substrate binding region based on the reported JMJD6 crystal structure (27, 28), suggesting that iJMJD6 may compete with α-KG and the substrate, but not Fe^{2+}, for binding. To test this, competition assays with increasing concentrations of α-KG, histone substrate, or Fe^{2+} were performed. The results showed that both α-KG and the substrate, but not Fe^{2+}, were able to compete with iJMJD6 for binding (Fig. 1*G*).

iJMJD6 Suppresses the Malignant Phenotypes of Multiple Types of Cancer Cells. We next sought to test the cytotoxicity of iJMJD6. Increasing evidence indicated that JMJD6 plays critical roles in cancer development, such as cervical cancer, hepatocellular carcinoma, and breast cancer, among others (17, 21–23, 29, 30). To examine its potency in these cancer cell lines, we first measured the physicochemical properties of iJMJD6, including its stability and protein binding capacity in cell culture medium as well as its permeability. The results showed that nearly 90% of iJMJD6 was intact 2 d after incubation with cell culture medium and maintained at a constant level even after 8 d (*SI Appendix*, Fig. S2*A*). Meanwhile, a relatively low percentage of iJMJD6 (29.4%) was found to bind with proteins in culture medium (*SI Appendix*, Fig. S2*B*). Furthermore, it could readily permeate Caco-2 cells, with an apparent permeability coefficient (Papp) of 11.09×10^{-6} cm s^{-1}. These data suggest that iJMJD6 has desirable, drug-like physicochemical properties.

We then examined the cytotoxicity of iJMJD6 in HeLa, SMCC7721, and MCF7 cells, representing cervical cancer, liver cancer, and breast cancer, respectively, through a cell proliferation assay. The half-maximum effective concentration (EC_{50}) of iJMJD6 in HeLa, SMCC7721, and MCF7 cells was 1.49, 9.37, and 9.53 μM, respectively (Fig. 2*A* and *SI Appendix*, Fig. S2 *C–E*). More importantly, iJMJD6 exhibited barely no cytotoxicity in normal cervical (Ect1/E6E7), liver (LO2), and breast epithelial cells (MCF10A), indicating that iJMJD6 is specific in killing cancer cells (*SI Appendix*, Fig. S2 *F–H*). The expression of JMJD6 was nearly undetectable in Ect1/E6E7, LO2, or MCF10A cells, while it was significantly increased in HeLa, SMCC7721, and MCF7 cancer cells, suggesting that iJMJD6 sensitivity is linked to the expression of JMJD6 in cells (*SI Appendix*, Fig. S2 *I* and *J*). We also examined the cytotoxicity of iJMJD6 in rapidly growing cells, such as endometrial stem cells. The EC_{50} of iJMJD6 was 100.5 μM, which is almost 70-fold higher than that in HeLa cells (*SI Appendix*, Fig. S2*K*).

We next investigated the effects of iJMJD6 on the malignant behaviors of cancer cells. Before this, we confirmed the functional role of JMJD6 in promoting the malignant behaviors of cancer cells. Specifically, we demonstrated that knockdown JMJD6 decreased the proliferation rate of HeLa cells (*SI Appendix*, Fig. S3 *A–C*). The effects of JMJD6 on cell proliferation were confirmed in JMJD6 knockout (KO) cells (*SI Appendix*, Fig. S3 *D–F*). JMJD6 knockout also induced cell cycle arrest at G0/G1

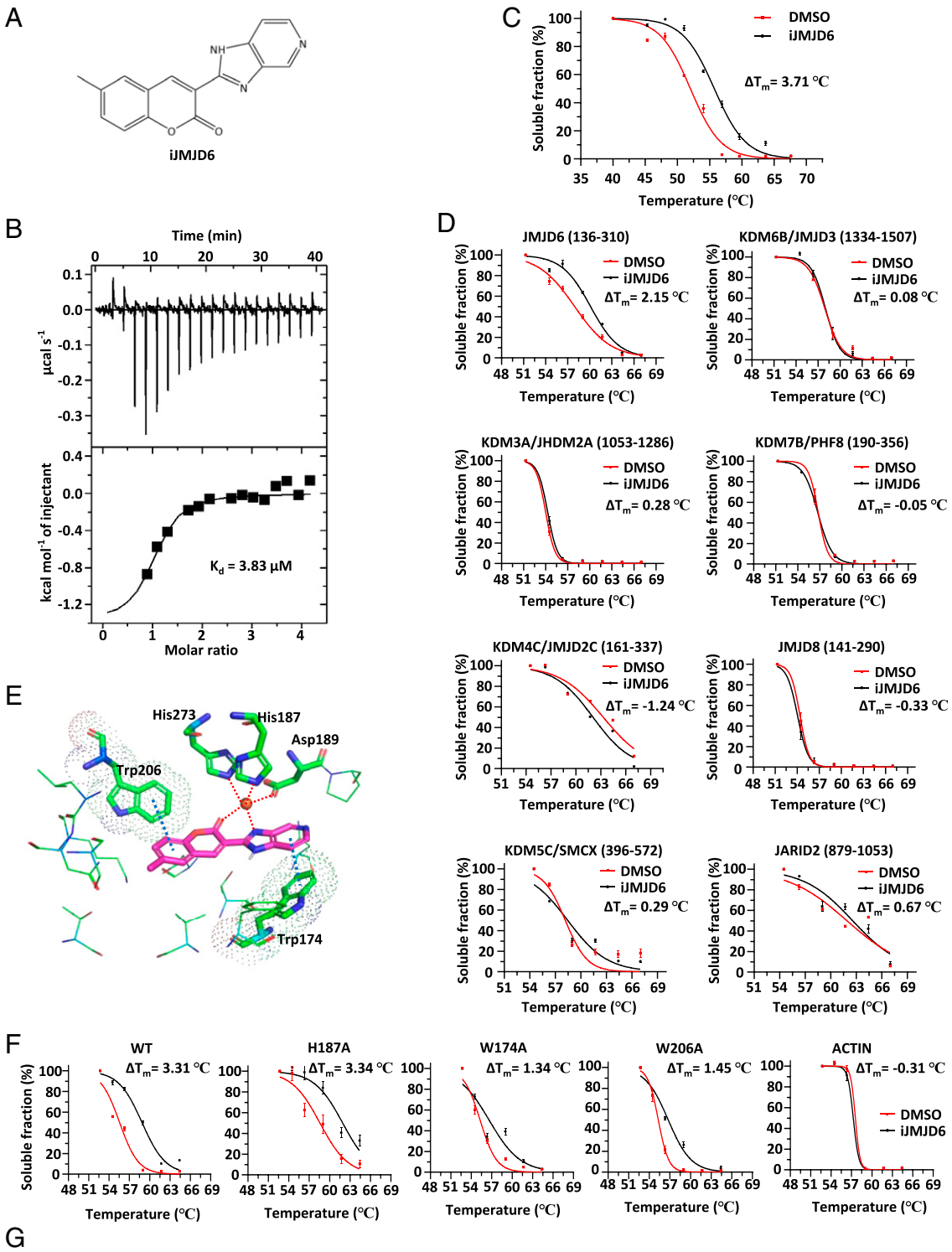

G

Substrate/ Cofactor	α-KG			Substrate			Fe^{2+}		
	0.5×	1×	2×	0.5×	1×	2×	0.5×	1×	2×
IC_{50} (μM)	0.0582	0.2376	0.317	0.058	0.2424	0.4301	0.2981	0.2989	0.2944

Fig. 1. iJMJD6 specifically binds to JMJD6 protein. (*A*) Chemical structure of iJMJD6. (*B*) iJMJD6 binding with JMJD6 was determined by isothermal titration calorimetry. The experiments were repeated three times and representative data are shown. (*C*) JMJD6 protein was incubated with dimethyl sulfoxide (DMSO) or iJMJD6 followed by thermal shift assay. JMJD6 protein versus temperature curve is shown. ΔT_m (difference between the denaturation temperature of JMJD6 protein in the presence and absence of iJMJD6). (*D*) The JmjC domain from members in the JmjC domain–containing demethylase protein family as indicated was incubated with DMSO or iJMJD6 followed by thermal shift assay. ΔT_m is shown. (*E*) Computational analysis of the binding mode of iJMJD6 with JMJD6 protein is shown (PDB ID: 3ldb). iJMJD6 is shown as magenta sticks. Amide acids are shown as green lines except that Trp206, Trp174, His187, Asp189, and His273 are highlighted with sticks. The surfaces of Trp206 and Trp174 are indicated by dots. The iron (Fe^{2+}) is shown as an orange sphere. The chelating bonds and the pi–pi interactions are shown as red and blue dashes, respectively. (*F*) WT JMJD6 or JMJD6 mutants with substitution of histidine 187 to alanine (H187A), tryptophan 174 to alanine (W174A), or tryptophan 206 to alanine (W206A) were incubated with or without iJMJD6 followed by cellular thermal shift assay (CETSA). Actin protein served as a negative control. (*G*) Demethylation assay was performed by mixing purified, bacterially expressed JMJD6 with core histones in the presence or absence of different concentrations of iJMJD6 followed by formaldehyde release measurement. Fe^{2+}, 1×, 20 μM $[NH_4]_2Fe[SO_4]_2$; α-KG, 1×, 1 mM α-ketoglutarate; and substrates, 1×, 5 μg. IC_{50} is shown.

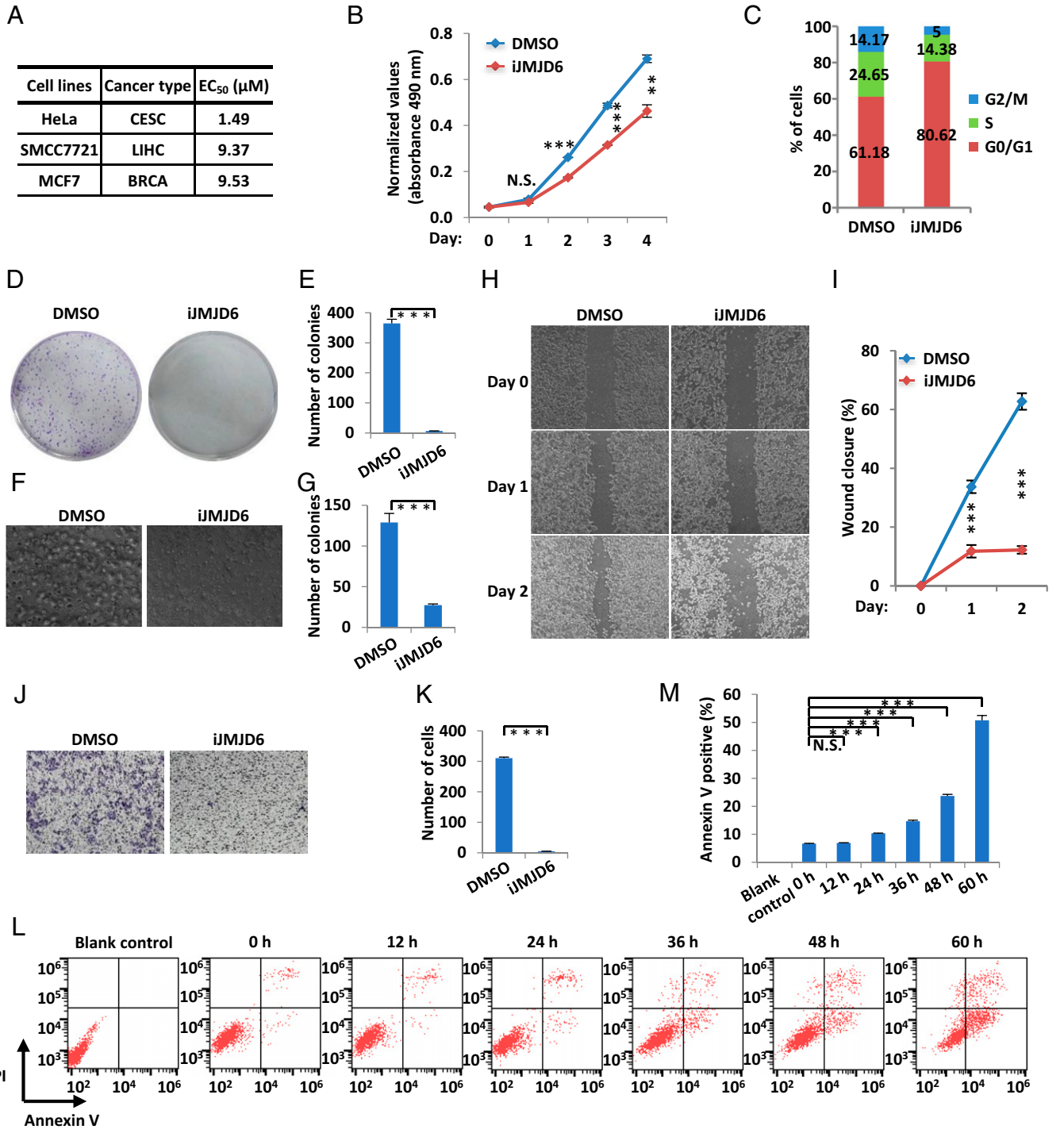

Fig. 2. iJMJD6 suppresses the malignant phenotypes of HeLa cervical cancer cells. (*A*) HeLa, SMCC7721, and MCF7 cells were treated with iJMJD6 at different concentrations for 72 h followed by cell proliferation assay. EC_{50} is shown. BRCA, breast invasive carcinoma; CESC, cervical squamous cell carcinoma and endocervical adenocarcinoma; LIHC, liver hepatocellular carcinoma. (*B–D*, *F*, *H*, *J*, and *L*) HeLa cells were treated with DMSO or iJMJD6 (1 μM) followed by cell proliferation assay (*B*) (±SEM; $^{**}P < 0.01$; $^{***}P < 0.001$; N.S., not significant), FACS analysis (*C*), colony formation assay (*D*), anchorage-independent growth assay (*F*), wound healing assay (*H*), Transwell assay (*J*), and apoptosis assay (*L*). Representative images are shown. (*E*, *G*, *I*, *K*, and *M*) Quantification of colony numbers (*E* and *G*), wound closure (*I*), migrated cells (*K*), and apoptotic cells (*M*) as shown in *D*, *F*, *H*, *J*, and *L*, respectively (±SEM; $^{***}P < 0.001$; N.S., not significant).

phase and suppressed colony formation, anchorage-independent growth, migration, and invasion in HeLa cells (*SI Appendix*, Fig. S3 *G–O*). JMJD6 knockout also induced apoptosis (*SI Appendix*, Fig. S3 *P* and *Q*). We then treated HeLa cells with iJMJD6 followed by a cell proliferation assay. Consistent with what we observed when knocking down JMJD6, iJMJD6 inhibited the proliferation of HeLa cells, induced cell cycle arrest at G0/G1 phase, and significantly impaired colony formation, anchorage-independent growth, migration, and invasion of HeLa cells (Fig. 2 *B–K*). iJMJD6 treatment also induced apoptosis in a time-dependent manner (Fig. 2 *L* and *M*). Similar effects of iJMJD6 were observed in SMCC7721 and MCF7 cells (*SI Appendix*, Figs. S4 and S5).

The Inhibitory Effects of iJMJD6 on Malignant Phenotypes in Cancer Cells Are Dependent on JMJD6. To validate the specificity of iJMJD6 in cancer cells, we tested the cytotoxicity of iJMJD6 in WT and JMJD6 KO HeLa cells. JMJD6 KO cells

were much less sensitive to iJMJD6 treatment, with an EC_{50} 100 times larger than that in wild-type HeLa cells (Fig. 3*A*). JMJD6 KO HeLa cells grew at a much slower rate than wild-type cells, which is in agreement with our previous results. Furthermore, JMJD6 KO cells were much less sensitive to iJMJD6 treatment compared to wild-type cells (Fig. 3*B*). As expected, JMJD6 knockout also significantly impaired G0/G1 transition, cell colony formation, anchorage-independent growth, and invasion (Fig. 3 *C–I*). More importantly, JMJD6 KO cells were not responsive to iJMJD6 treatment in these assays (Fig. 3 *C–I*). Similarly, JMJD6 knockout made HeLa cells inert to iJMJD6 treatment in apoptosis assays (Fig. 3 *J* and *K*). Taken together, the effects of iJMJD6 on the malignant phenotypes in cancer cells are dependent on JMJD6, supporting the targeting specificity of iJMJD6.

iJMJD6 Inhibits JMJD6-Mediated Demethylation Events to Inhibit the Expression of Oncogenes, Including Myc and CCND1 in Cancer Cells. We and others have reported that the functional importance of JMJD6 in cancer development was largely dependent on its enzymatic activity, particularly its arginine demethylase activity targeting histone as well as nonhistone proteins (10, 17, 21, 23, 29), to regulate the expression of a large set of oncogenes, such as c-Myc, N-myc, and CCND1 (19, 21, 23, 24, 30–34). We then focused on investigating the effects of iJMJD6 on JMJD6-mediated demethylation in cancer cells. Our previous study demonstrated that JMJD6 specifically and locally demethylates histone H4 arginine 3 symmetrical dimethylation [H4R3me2(s)] to activate gene expression (17). Indeed, the global level of H4R3me2(s) remained unchanged upon iJMJD6 treatment (*SI Appendix*, Fig. S6*A*). A significant increase of H4R3me2(s) occupancy was observed on JMJD6-bound genomic regions based on H4R3me2(s) chromatin immunoprecipitation sequencing (ChIP-seq) analysis, while minor changes on random genomic regions upon iJMJD6 treatment were observed (Fig. 4 *A–C*). We have also examined H3R17me2(a), a histone marker known to be unaffected by JMJD6 (9, 17), in the presence or absence of iJMJD6 in HeLa cells. The results demonstrated that the total levels of H3R17me2(a) were not changed upon iJMJD6 treatment (*SI Appendix*, Fig. S6*A*), and the occupancy of H3R17me2(a) was unchanged on JMJD6-bound chromatin regions or random genomic regions upon iJMJD6 treatment (*SI Appendix*, Fig. S6 *B* and *C*). It has also been reported that JMJD6 targets nonhistone proteins, such as HSP70, ERα, PAX3, DHX9, STAT1, TRAF6, and hnRNPA2B1, for demethylation (10–13, 15, 16, 25). For HSP70 protein, for which we have a methylation-specific antibody (15), iJMJD6 was found to induce the levels of HSP70R469me1 (arginine 469 monomethylation) in a time-dependent manner (*SI Appendix*, Fig. S6 *D–F*). The increase of HSP70R469me1 by iJMJD6 was JMJD6 dependent, as JMJD6 knockout cells were unresponsive to iJMJD6 treatment (*SI Appendix*, Fig. S6*G*). These data suggest that iJMJD6 specifically targets JMJD6 to inhibit JMJD6-mediated demethylation.

JMJD6 was also known as a α-KG–dependent hydroxylase, catalyzing lysyl C-5 hydroxylation of histone H4, histone H3, and U2AF65 proteins (35). JMJD6 hydroxylates H4, H3, and U2AF65 peptides, which were not affected by iJMJD6, even at a concentration of 10 μM as seen from both matrix-assisted laser desorption/ionization-time-of-flight mass spectrometry (MALDI-TOF MS) analysis and Succinate-Glo assay (*SI Appendix*, Fig. S7 *A–C*). However, our previous data demonstrated that iJMJD6 is capable of inhibiting the demethylase activity of JMJD6 with a IC_{50} of 149.6 ± 34.1 nM.

We next tested whether iJMJD6 inhibits the expression of oncogenes, including c-Myc, N-myc, and CCND1. The requirement of JMJD6 for the expression of c-Myc, N-myc, and CCND1 was first confirmed in HeLa cells (Fig. 4 *D* and *E*). Consistently, iJMJD6 treatment led to a significant decrease of c-Myc, N-myc, and CCND1 in a time-dependent manner (Fig. 4 *F* and *G*). Furthermore, the inhibitory effects of iJMJD6 on the expression of these genes was dependent on JMJD6 (Fig. 4*H*). The effects of JMJD6 knockdown as well as iJMJD6 on the expression of c-Myc, N-myc, and CCND1 were independently confirmed in SMCC7721 and MCF7 cells (*SI Appendix*, Fig. S8 *A–H*).

To link the inhibitory effects of iJMJD6 on JMJD6-mediated demethylation with its inhibitory effects on oncogene expression, H4R3me2(s) occupancy was found to be increased significantly on JMJD6-bound enhancers near c-Myc, N-myc, and CCND1 (Fig. 4*I*), while minor changes were observed for regions 5 kb upstream of translation start sites and 5 kb downstream of translation terminal sites, where no JMJD6 binding was detected (*SI Appendix*, Fig. S8*I*). To determine whether the histone modification change is a cause or consequence of the transcriptional change, we performed time-course experiments to examine the occupancy of H4R3me2(s) and the expression of c-Myc, N-myc, and CCND1 upon iJMJD6 treatment. The results showed that the induction of H4R3me2(s) occupancy often occurred before transcriptional repression in the presence of iJMJD6 (Fig. 4 *J* and *K*). For instance, H4R3me2(s) occupancy was slightly increased at 0.5 h and peaked at 3 h on N-myc, while the mRNA levels of N-myc started to decrease at 3 h after iJMJD6 treatment (Fig. 4 *J* and *K*). Similarly, for CCND1, H4R3me2(s) occupancy was slightly increased at 0.5 h and peaked at 1 h, while its mRNA levels started to decrease after 1 h upon iJMJD6 treatment (Fig. 4 *J* and *K*). For c-Myc, H4R3me2(s) occupancy peaked as early as 0.5 h, when a corresponding decrease of mRNA levels was already seen (Fig. 4 *J* and *K*). These data suggest that iJMJD6 might inhibit the transcription of these oncogenes through inhibiting JMJD6-mediated demethylation of H4R3me2(s).

We next sought to investigate whether JMJD6 target genes, such as c-Myc and CCND1, are involved in iJMJD6-mediated inhibition in HeLa cells. It was found that both c-Myc and CCND1 rescued the defects caused by iJMJD6 treatment in cell proliferation, cell cycle progression, and cell migration (*SI Appendix*, Fig. S9 *A–E*). Thus, iJMJD6 inhibits the expression of oncogenes, including Myc and CCND1, by specifically targeting JMJD6, which could account for its inhibitory effects on the malignant phenotypes of cancer cells.

iJMJD6 Exhibits Potent Antiumor Activity in Cell Line– and Patient-Derived Xenograft Mouse Models. We next examined the antitumor activity of iJMJD6 in xenograft mouse models. To this end, we first examined the pharmacokinetic properties of iJMJD6 in mice. iJMJD6 was still detectable in the plasma even 1 d after intravenous or oral administration (*SI Appendix*, Fig. S10*A*). The half-life of iJMJD6 was 2.332 h when it was intravenously administrated. When orally administrated, iJMJD6 was rapidly absorbed with a T_{max} of 0.5 h, a half-life of 6.683 h, and a mean residence time of 1.287 h (*SI Appendix*, Fig. S10*B*). The absolute oral bioavailability was 53.16%. These data suggested that iJMJD6 exhibits a favorable pharmacokinetic profile for in vivo study. We next assessed the safety of iJMJD6. To this end, mice were treated with iJMJD6 at the dose of 25 or 50 mg/kg every other day for 28 d. Mice were able to tolerate well these dosages that were effective in tumor suppression (see below), exhibiting no evidence of abnormality in complete

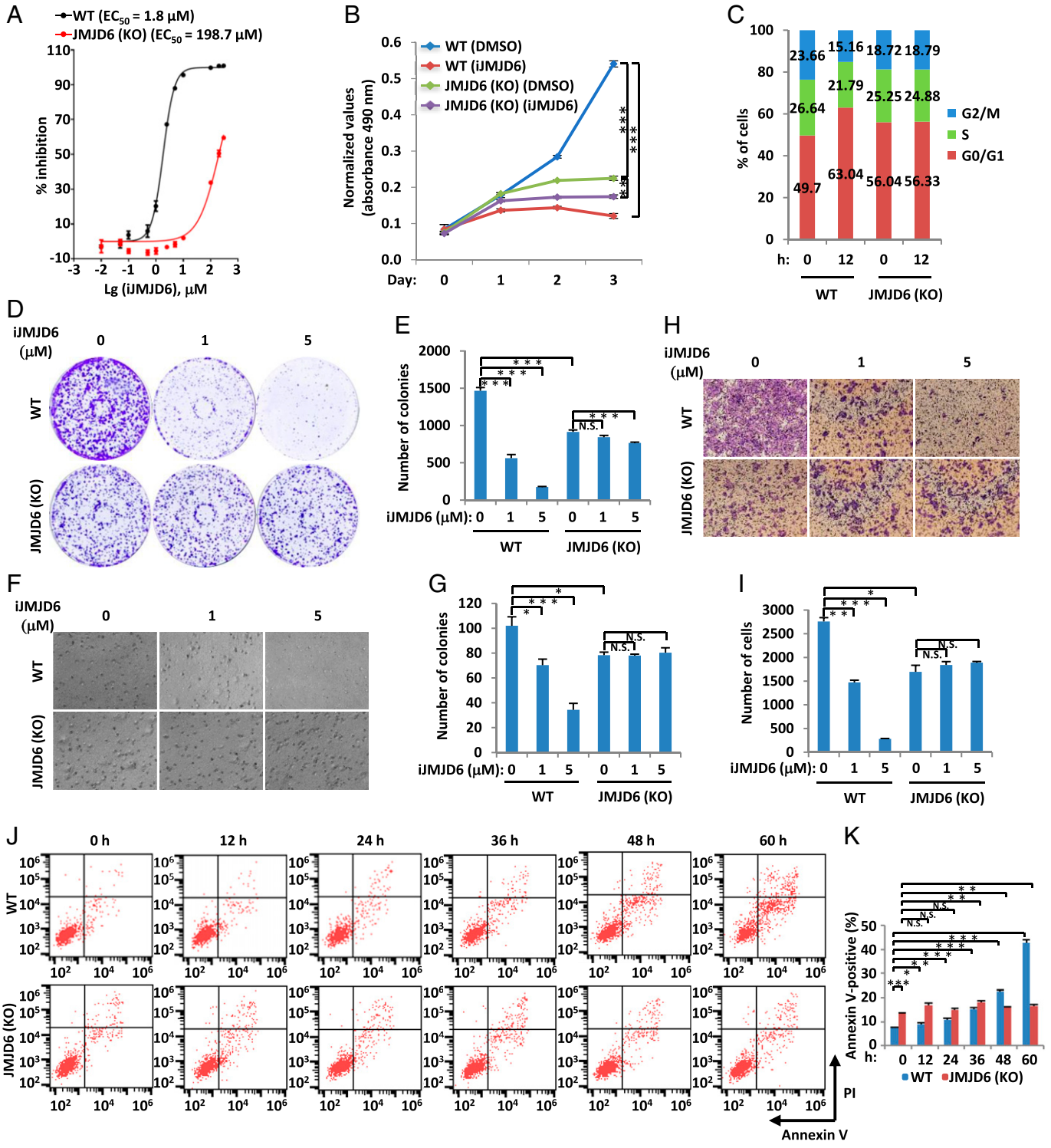

Fig. 3. The inhibitory effects of iJMJD6 on the malignant phenotypes in HeLa cells are dependent on JMJD6. (*A*) WT and JMJD6 KO HeLa cells were treated with iJMJD6 at concentrations as indicated for 72 h followed by cell proliferation assay. EC_{50} is shown. (*B–D*, *F*, *H*, and *J*) WT and JMJD6 KO HeLa cells were treated with DMSO or iJMJD6 (1 μM) unless otherwise stated, followed by cell proliferation assay (*B*) (±SEM; $^{**}P < 0.01$; $^{***}P < 0.001$), FACS analysis (*C*), colony formation assay (*D*), anchorage-independent growth assay (*F*), Transwell assay (*H*), and apoptosis assay (*J*). Representative images are shown. (*E*, *G*, *I*, and *K*) Quantification of colony numbers (*E* and *G*), migrated cells (*I*), and apoptotic cells (*K*) as shown in *D*, *F*, *H*, and *J*, respectively (±SEM; $^{*}P < 0.05$; $^{**}P < 0.01$; $^{***}P < 0.001$; N.S., not significant).

blood count analysis (*SI Appendix*, Fig. S10*C*), comprehensive metabolic panel analysis (*SI Appendix*, Fig. S10*D*), the size/weight of various organs (*SI Appendix*, Fig. S10 *E* and *G*), or histological analysis (*SI Appendix*, Fig. S10*F*).

iJMJD6 treatment significantly suppressed the growth of HeLa cell–derived xenografts, as evidenced by the decreased tumor size, weight, and cell density from hematoxylin and eosin (H&E) staining of tumor sections (Fig. 5 *A* and *B* and *SI Appendix*, Fig. S11*A*). The expression of c-Myc, N-myc, and CCND1 was significantly lower in tumors treated with iJMJD6 than the control ones (Fig. 5*C*). No weight lost was detected when mice were treated with iJMJD6 (*SI Appendix*, Fig. S11*B*).

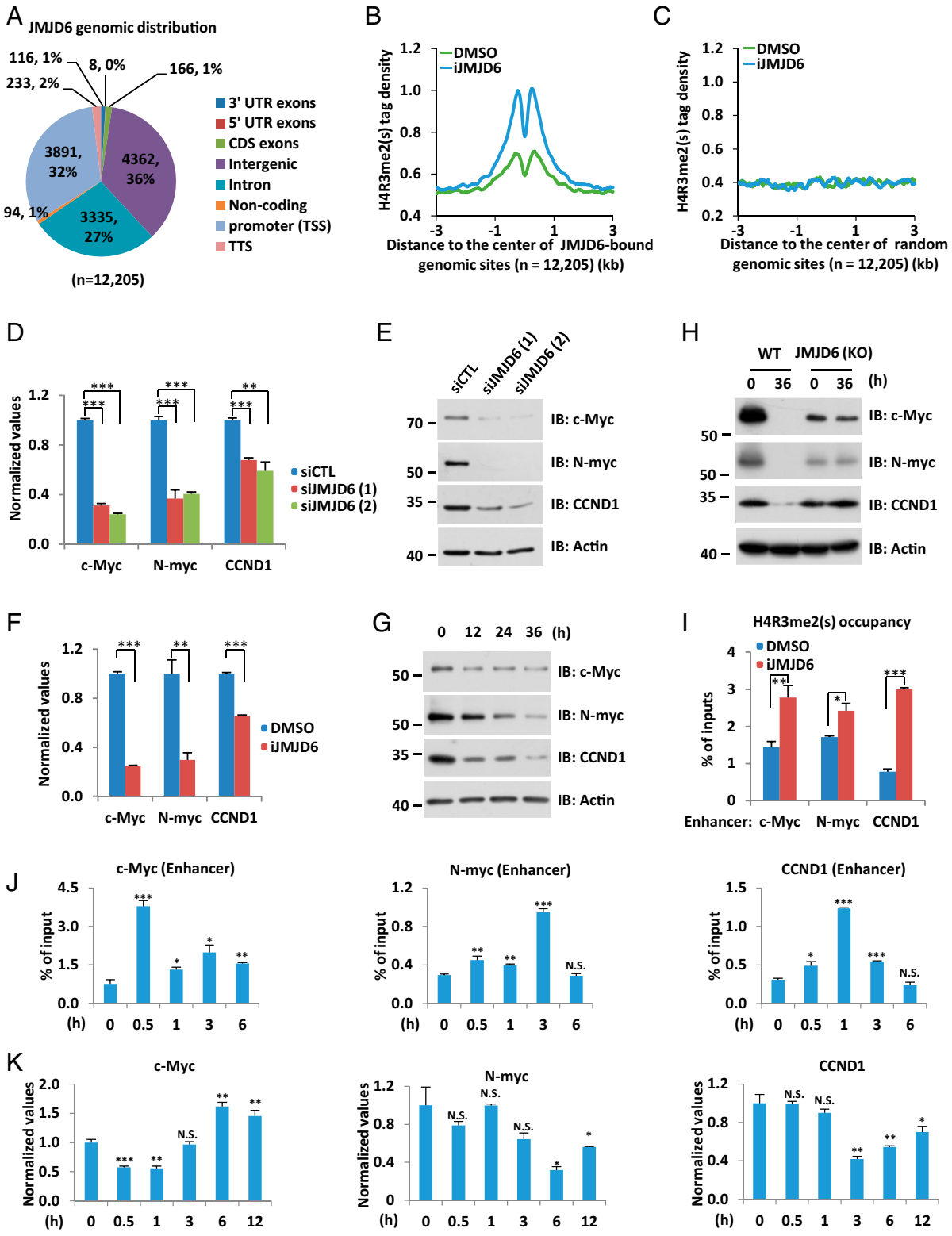

Fig. 4. iJMJD6 inhibits JMJD6-mediated demethylation to inhibit the expression of Myc and CCND1 in HeLa cells. (*A*) JMJD6 ChIP-seq was performed in HeLa cells, and the genomic distribution of JMJD6 binding sites is shown by pie chart. (*B* and *C*) HeLa cells were treated with or without iJMJD6 (1 μM) for 1 h followed by H4R3me2(s) ChIP-seq; and the ChIP-seq tag distribution surrounding the center of JMJD6-bound (*B*) or random genomic sites (*C*) is shown. (*D* and *E*) HeLa cells were transfected with control siRNA (siCTL) or two independent siRNAs specifically targeting JMJD6 (siJMJD6 [1] and siJMJD6 [2]) followed by RT-qPCR (*D*) and immunoblotting (IB) (*E*) analysis to examine the mRNA and protein levels of c-Myc, N-Myc, and CCND1, respectively (±SEM; $^{**}P < 0.01$; $^{***}P < 0.001$). (*F* and *G*) HeLa cells were treated with or without iJMJD6 (1 μM) followed by RT-qPCR (*F*) and IB (*G*) analysis to examine the mRNA and protein levels of c-Myc, N-Myc, and CCND1, respectively (±SEM; $^{**}P < 0.01$; $^{***}P < 0.001$). (*H*) WT and JMJD6 KO HeLa cells were treated with or without iJMJD6 (1 μM) for 36 h followed by IB with antibodies as indicated. (*I*) HeLa cells were treated with or without iJMJD6 (1 μM) for 1 h followed by H4R3me2(s) ChIP, and the occupancy of H4R3me2(s) on the enhancer regions of genes as indicated is shown. ChIP signals are presented as % of inputs (±SEM; $^{*}P < 0.05$; $^{**}P < 0.01$; $^{***}P < 0.001$). (*J*) HeLa cells were treated with or without iJMJD6 (1 μM) for the duration as indicated followed by H4R3me2(s) ChIP, and the occupancy of H4R3me2(s) on the enhancer regions of genes as indicated is shown. ChIP signals are presented as % of inputs (±SEM; $^{*}P < 0.05$; $^{**}P < 0.01$; $^{***}P < 0.001$; N.S., not significant). (*K*) HeLa cells were treated with or without iJMJD6 (1 μM) for the duration as indicated followed by RT-qPCR analysis for genes as indicated (±SEM; $^{*}P < 0.05$; $^{**}P < 0.01$; $^{***}P < 0.001$; N.S., not significant).

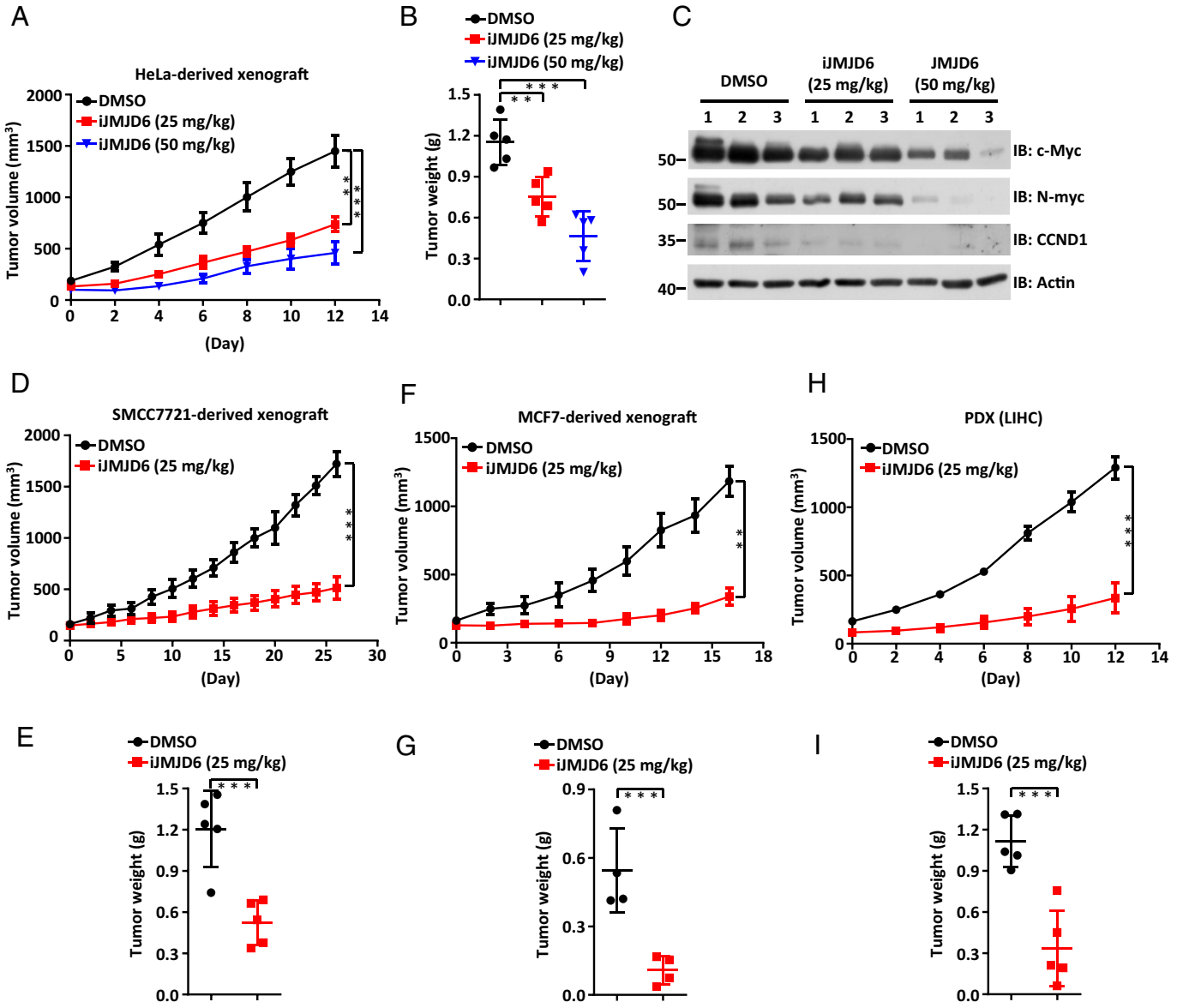

Fig. 5. iJMJD6 exhibits potent antitumor activity in cancer cell line– and patient-derived xenograft mouse models. (*A*, *D*, and *F*) Female BALB/c nude mice were inoculated with HeLa (*A*), SMCC7721 (*D*), or MCF7 (*F*) cells, randomized, treated with DMSO or iJMJD6 at dosages as indicated intraperitoneally (i.p.) every other day. Tumor growth curve is shown (±SEM; $^{**}P < 0.01$; $^{***}P < 0.001$). (*B*, *E*, and *G*) The weight of tumors as described in *A*, *D*, and *F* is shown in *B*, *E*, and *G* (±SEM; $^{**}P < 0.01$; $^{***}P < 0.001$). (*C*) Representative tumor samples as described in *A* were subjected to IB analysis with antibodies as indicated. (*H*) BALB/c nude mice were implanted with tumor fragments from liver cancer PDXs, randomized, and treated with DMSO or iJMJD6 at dosages as indicated intraperitoneally every other day. Tumor growth curve is shown (±SEM; $^{***}P < 0.001$). (*I*) The weight of tumors as described in *H* is shown (±SEM; $^{***}P < 0.001$).

iJMJD6 also significantly inhibited the growth of SMCC7721- and MCF7-derived xenografts (Fig. 5 *D*–*G*). The antitumor activity of iJMJD6 was also observed in liver cancer PDXs treated with iJMJD6 (Fig. 5 *H* and *I*). JMJD6 has also been implicated in the development of triple negative breast cancer (TNBC), glioblastoma (GBM), and colorectal cancer (CRC), among others (19, 30, 32). iJMJD6 significantly suppressed the growth of MDA-MB-231 (TNBC)-, U87 (GBM)-, and HCT116 (CRC)-derived xenografts (*SI Appendix*, Fig. S11 *C*–*H*). Similarly, TNBC, GBM, and CRC PDXs were significantly suppressed by iJMJD6 in mice (*SI Appendix*, Fig. S11 *I*–*N*). In summary, these data suggest that iJMJD6 is effective and safe for treatment in vivo in xenograft mouse models.

Combination Therapy with iJMJD6 and BRD4 Inhibitor JQ1 Exhibits Synergistic Effects on Suppressing Tumor Growth. We and others have reported that JMJD6 interacts with BRD4 to regulate a large number of genes with implications in cancer development, including Myc and CCND1 (17, 36). We therefore tested whether combination therapy with iJMJD6 and JQ1, a well-studied BRD4 inhibitor, improves the efficacy of iJMJD6 in tumor suppression. We first demonstrated that the expression of c-Myc, N-myc, and CCND1 were drastically down-regulated in HeLa cells that were cotreated with iJMJD6 and JQ1 (Fig. 6*A*). Consistently, cotreatment with iJMJD6 and JQ1 exhibited synergistic effects on cell proliferation, cell cycle progression, colony formation, anchorage-independent growth, migration, invasion, and apoptosis in HeLa cells (Fig. 6 *B*–*M*). The synergistic effects of iJMJD6 and JQ1 on Myc and CCND1 expression as well as cell proliferation were also observed in SMCC7721 and MCF7 cells (*SI Appendix*, Fig. S12 *A* and *B*). We further tested the antitumor effects of combination therapy in a HeLa cell–derived xenograft mouse model. While the tumor suppressive effects of iJMJD6 or JQ1 were readily seen, the combination of

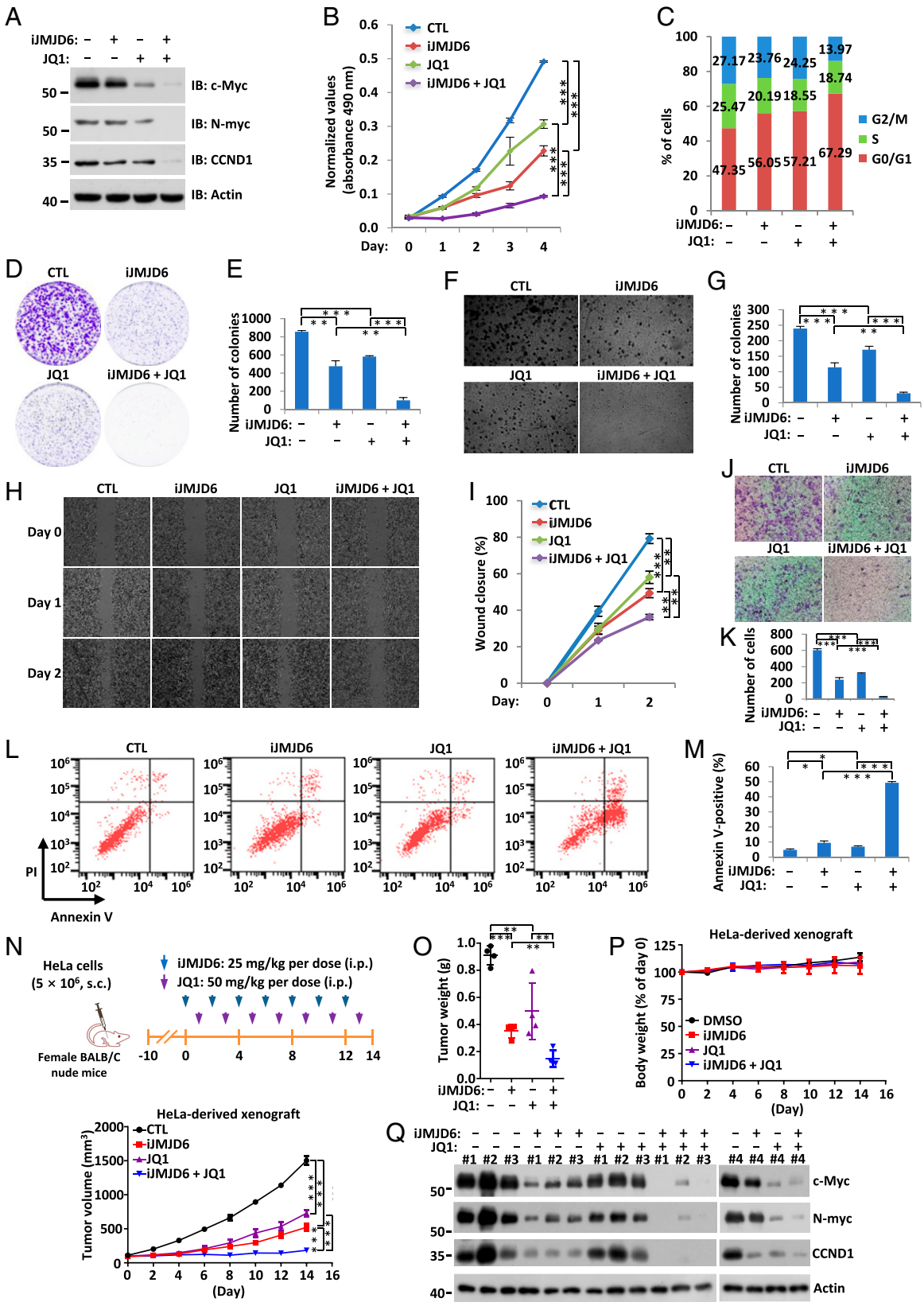

Fig. 6. Combination therapy with iJMJD6 and JQ1 exhibits synergistic effects on tumor growth. (*A*) HeLa cells were treated with iJMJD6 (0.5 μM) or JQ1 (2.5 μM) alone or in combination for 12 h, followed by IB with antibodies as indicated. (*B–D, F, H, J,* and *L*) HeLa cells were treated with iJMJD6 (0.5 μM) or JQ1 (2.5 μM) alone or in combination, followed by cell proliferation assay (*B*) (±SEM; ***$P < 0.001$), FACS analysis (*C*), colony formation assay (*D*), anchorage-independent growth assay (*F*), wound healing assay (*H*), Transwell assay (*J*), and apoptosis assay (*L*). Representative images are shown. (*E, G, I, K,* and *M*) Quantification of colony numbers (*E* and *G*), wound closure (*I*), migrated cells (*K*), and apoptotic cells (*M*) as shown in *D, F, H, J,* and *L*, respectively (±SEM; *$P < 0.05$; **$P < 0.01$; ***$P < 0.001$). (*N*) Female BALB/c nude mice ($n = 16$) were inoculated with HeLa cells, randomized, and treated with iJMJD6 (25 mg/kg) or JQ1 (50 mg/kg) alone or in combination at dosages as indicated intraperitoneally every other day. Experimental design and tumor growth curve are shown (±SEM; ***$P < 0.001$). s.c., subcutaneous injection; i.p., intraperitoneal injection. (*O*) The weight of tumors as described in *N* is shown (±SEM; **$P < 0.01$; ***$P < 0.001$). (*P*) The body weight of mice as described in *N*. (*Q*) Tumor samples as described in *N* were subjected to IB analysis with antibodies as indicated.

iJMJD6 and JQ1 showed a synergistic effect (Fig. 6 *N* and *O*). There was no significant difference in body weight of mice in the different groups, indicating that the combination therapy is well tolerated (Fig. 6*P*). Importantly, combination therapy with iJMJD6 and JQ1 drastically repressed the expression of c-Myc, N-myc, and CCND1 compared to either treatment alone, linking the inhibitory role of iJMJD6 and JQ1 in gene transcription with their antitumor activity (Fig. 6*Q*). Overall, these results suggest the combination therapy with iJMJD6 and BRD4 inhibitor JQ1 is advantageous in suppressing tumor growth than either alone.

Combination Therapy with iJMJD6 and ERα Degrader Fulvestrant (ICI) Improves the Efficacy of ICI in Suppressing ERα-Positive Breast Cancer. We have reported previously that JMJD6 is specifically recruited to ERα-bound enhancers and cooperate with ERα to activate estrogen-target genes, including Myc and CCND1, and promote ERα-positive breast tumor growth (21). To extend the potential value of iJMJD6 in the clinic, we examined whether combination therapy with iJMJD6 and ER degrader fulvestrant (ICI), the first-line drug used for treating ER-positive breast cancer, will improve the efficacy of ICI in suppressing ER-positive breast tumor growth. As expected, iJMJD6 greatly improved the efficacy of ICI in suppressing the expression of c-Myc, N-myc, and CCND1 in MCF7 cells (Fig. 7*A*). Consistently, iJMJD6 cotreatment greatly potentiates the effects of ICI in suppressing cell proliferation, cell cycle progression, colony formation, anchorage-independent growth, migration, and invasion in MCF7 cells (Fig. 7 *B*–*K*). The synergistic effects of iJMJD6 and ICI on the expression of Myc and CCND1 as well as cell proliferation was also observed in another ERα-positive breast cancer cell line, T47D (*SI Appendix*, Fig. S13 *A* and *B*). Consistent with what was observed in cultured cells, iJMJD6 significantly improved the efficacy of ICI in suppressing tumor growth (Fig. 7 *L* and *M*). Exogenous administration of estrogen was to sustain the growth of tumor in mice. The body weight of mice showed no significant difference (Fig. 7*N*). The expression of c-Myc, N-myc, and CCND1 was drastically decreased in tumors cotreated with iJMJD6 and ICI (Fig. 7*O*). Taken together, these results suggest the combination therapy with iJMJD6 and ERα degrader ICI improves the efficacy of ICI in suppressing ERα-positive breast cancer.

Discussion

JMJD6 has been demonstrated to be a drug target with great potential in multiple types of cancers. However, no small-molecule inhibitors specifically targeting JMJD6 with potent antitumor activity have been reported so far. Here, we demonstrated that iJMJD6, a specific JMJD6 inhibitor, has favorable physicochemical and pharmacokinetic properties and is potent in suppressing the growth of multiple types of cancer cells both in vitro and in vivo.

We sought to characterize the binding mode between iJMJD6 and JMJD6 protein. Computational modeling and experimental validation results revealed that iJMJD6 competes with the α-KG cofactor and substrate, but not Fe^{2+}, for binding with JMJD6. The capacity of iJMJD6 to interfere with the binding of both α-KG and the substrate might account for its better activity and specificity over other α-KG mimics. Future study to solve the crystal structure between iJMJD6 and JMJD6 protein will help us to better understand the binding mode and facilitate the optimization toward more potent and selective JMJD6 inhibitors.

JMJD6 possesses multiple enzymatic activities, including arginine demethylase, lysine hydroxylase, protein clipping, and tyrosine kinase activity (9, 28, 35, 37). The active center of JMJD6 is essential for its arginine demethylase, lysine hydroxylase, and clipping activities, while it is unclear which domain is responsible for the tyrosine kinase activity. The substrate binding regions for methylated arginine, lysine, and clipping site are supposed to be quite different in JMJD6, through which iJMJD6 might be able to achieve its specificity. The diverse enzymatic activities of JMJD6 are linked to its diverse biological functions. For instance, JMJD6-mediated lysine hydroxylation of splicing factor U2AF65 is known to regulate its function in gene alternative splicing (20, 35), while JMJD6-mediated histone demethylation has been demonstrated to be critical for gene transcriptional activation (9, 10, 13, 14, 17, 21, 23, 29). We found that the hydroxylation activity of JMJD6 on H4, H3, and U2AF65 peptides was not affected by iJMJD6 even at a concentration of 10 μM. However, our previous data demonstrated that iJMJD6 is capable of inhibiting the arginine demethylase activity of JMJD6 with an IC_{50} of 149.6 ± 34.1 nM. iJMJD6 therefore preferentially targets the demethylase activity of JMJD6. We then focused on examining iJMJD6 effects on JMJD6 demethylase activity and JMJD6-regulated gene transcription in cancer cells. iJMJD6 treatment, similar to JMJD6 knockdown, led to a significant increase of H4R3me2(s) occupancy on the enhancers of c-Myc, N-myc, and CCND1, where JMJD6 binds. Consistent with previous findings that JMJD6 regulates the expression of oncogenes such as c-Myc and CCND1 to promote tumorigenesis, iJMJD6 was found to effectively inhibit the expression of these genes and the growth of multiple types of cancer cells. Myc and CCND1 can partially rescue the growth inhibition caused by iJMJD6 treatment in HeLa cells. However, the exact substrate(s) through which iJMJD6 works to inhibit cancer cell growth remains to be determined, but we are certain that H4R3me2(s), if not the only, is at least one of the most important ones. It should be noted that JMJD6 is involved in a plethora of cellular pathways, including TBK1-IFR3 (16), JAK-STAT (13), P53 (32), TGFβ (22), and Wnt/β-catenin pathways (25). iJMJD6 could serve as a great tool to assess the involvement of JMJD6 enzymatic activity in these cellular pathways, facilitating our further understanding of the underlying molecular mechanisms.

The suitable pharmacokinetics of iJMJD6 prompted us to further test the antitumor activity of iJMJD6 in vivo. iJMJD6 exhibits potent tumor-suppressive activities in a number of cancer cell line– and patient-derived xenograft mouse models safely. Combination therapy has been proved to be an effective way of treating cancers in the clinic. Based on the molecular mechanisms through which JMJD6 regulates gene transcription and the malignant behaviors of cancer cells, it is worthy of exploring therapeutic strategies to combine iJMJD6 with other antitumor agents/drugs. We demonstrated here that cotreatment of iJMJD6 and BET inhibitor JQ1 or ICI exhibited synergistic effects in tumor suppression. As discussed above, JMJD6 is implicated in various signaling pathways, which warrants future study to investigate the therapeutic effects of combining iJMJD6 with inhibitors or drugs targeting these pathways.

In conclusion, iJMJD6 is a specific JMJD6 inhibitor that potently suppresses tumorigenesis safely in mice. Combination therapy with iJMJD6 and other antitumor agents, such as JQ1 and ICI, exhibits synergistic effects in tumor suppression. iJMJD6 therefore might serve as a great tool for further exploring JMJD6 function in both physiological and pathological processes and provide a therapeutic avenue for treating cancers that are dependent on JMJD6 in the clinic.

Materials and Methods

Detailed materials and methods are available in *SI Appendix*. This includes the following: plasmids and cloning procedures, siRNAs, antibodies, compounds,

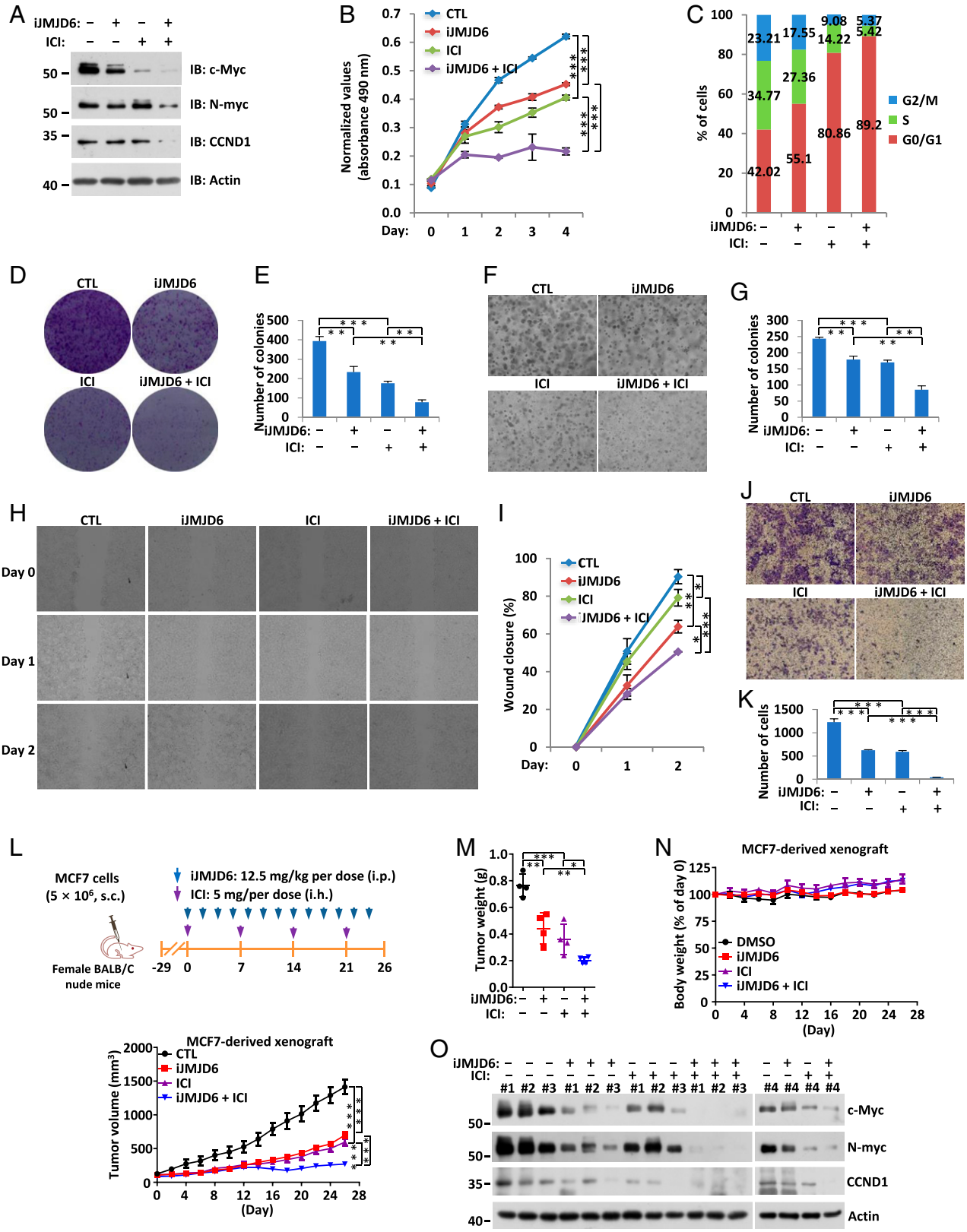

Fig. 7. Combination therapy with iJMJD6 and ICI improves the efficacy of ICI in suppressing ERα-positive breast cancer. (*A*) MCF7 cells were treated with iJMJD6 (5 μM) or ICI (fulvestrant, 2 μM) alone or in combination for 12 h, followed by IB with antibodies as indicated. (*B–D*, *F*, *H*, and *J*) MCF7 cells were treated with iJMJD6 (5 μM) or ICI (2 μM) alone or in combination, followed by cell proliferation assay (*B*) (±SEM; ***$P < 0.001$), FACS analysis (*C*), colony formation assay (*D*), anchorage-independent growth assay (*F*), wound healing assay (*H*), and Transwell assay (*J*). Representative images are shown. (*E*, *G*, *I*, and *K*) Quantification of colony numbers (*E* and *G*), wound closure (*I*), and migrated cells (*K*) as shown in *D*, *F*, *H*, and *J*, respectively (±SEM; *$P < 0.05$; **$P < 0.01$; ***$P < 0.001$). (*L*) Female BALB/c nude mice ($n = 16$) were inoculated with MCF7 cells, brushed with or without estrogen (E_2, 0.01 M) on the neck every 3 d, randomized, and treated with iJMJD6 (12.5 mg/kg, every other day) or ICI (5 mg/wk) alone or in combination at dosages as indicated intraperitoneally. Experimental design and tumor growth curve are shown (±SEM; ***$P < 0.001$). s.c., subcutaneous injection; i.p., intraperitoneal injection; i.h., injectio hypodermica. (*M*) The weight of tumors as described in *L* is shown (±SEM; *$P < 0.05$; **$P < 0.01$; ***$P < 0.001$). (*N*) The body weight of mice as described in *L*. (*O*) Tumor samples as described in *L* were subjected to IB analysis with antibodies as indicated.

in vitro demethylation assay and formaldehyde release assay, in vitro hydroxylation assay followed by MALDI-TOF MS analysis and Succinate-Glo assay, immunoblotting assay, isothermal titration calorimetry, differential scanning calorimetry, thermal shift assay, measurement of the protein binding activity of iJMJD6 in cell culture media, measurement of the stability of iJMJD6 in cell culture medium, measurement of cell permeability of iJMJD6, generation of JMJD6 knockout cell lines using CRISPR-Cas9 gene editing technology, cell proliferation assay, colony formation assay, anchorage-independent growth assay, wound healing assay, Transwell assay, fluorescence-activated cell sorting (FACS) analysis, apoptosis assay, RNA isolation and RT-qPCR, pharmacokinetics, drug safety assessment, xenograft tumor assay, ChIP-seq and data analysis, and compound synthesis.

Mice. Mice were purchased from Beijing Vital River Laboratory Animal Technology and maintained in an animal room with 12-h light/12-h dark cycles at the animal facility at Xiamen University under pathogen-free conditions. All of the animal experiments were approved by the animal care and use committee of Xiamen University.

Data, Materials, and Software Availability. All ChIP-seq data were deposited in the GEO database under accession GSE201988 (38). All other study data are included in the article and/or *SI Appendix*.

ACKNOWLEDGMENTS. This work was supported by the Ministry of Science and Technology of China (2020YFA0112300 and 2020YFA0803600), the National Natural Science Foundation of China (82125028, 91953114, 31871319, 81861130370, and 81761128015), the Natural Science Foundation of Fujian Province of China (2020J02004), and the Fundamental Research Funds for Central University (20720190145 and 20720220003) (to W.L.). This work was also supported by the China Postdoctoral Science Foundation (2020M682088) (to R.-q.X.). We thank Dr. Cai-sheng Wu for discussions on pharmacokinetics study, Dr. Xiang Gao for technical assistance on the MALDI-TOF MS experiments, Dr. Xiao-sheng Yan for technical assistance on absorption and fluorometric measurements, Drs. Jia-bian Lian and Lu Xia for providing CRC PDXs, Dr. Zhi-qian Zhang for providing liver hepatocellular carcinoma PDXs, Dr. Su-ling Liu for providing TNBC PDXs, and Dr. Cheng-hao Huang for providing GBM PDXs.

1. A. J. Bannister, T. Kouzarides, Regulation of chromatin by histone modifications. *Cell Res.* **21**, 381–395 (2011).
2. J. Murn, Y. Shi, The winding path of protein methylation research: Milestones and new frontiers. *Nat. Rev. Mol. Cell Biol.* **18**, 517–527 (2017).
3. M. T. Pedersen, K. Helin, Histone demethylases in development and disease. *Trends Cell Biol.* **20**, 662–671 (2010).
4. Y. Cheng *et al.*, Targeting epigenetic regulators for cancer therapy: Mechanisms and advances in clinical trials. *Signal Transduct. Target. Ther.* **4**, 62 (2019).
5. N. R. Rose *et al.*, Inhibitor scaffolds for 2-oxoglutarate-dependent histone lysine demethylases. *J. Med. Chem.* **51**, 7053–7056 (2008).
6. L. Wang *et al.*, A small molecule modulates Jumonji histone demethylase activity and selectively inhibits cancer growth. *Nat. Commun.* **4**, 2035 (2013).
7. L. Kruidenier *et al.*, A selective jumonji H3K27 demethylase inhibitor modulates the proinflammatory macrophage response. *Nature* **488**, 404–408 (2012).
8. V. A. Fadok *et al.*, A receptor for phosphatidylserine-specific clearance of apoptotic cells. *Nature* **405**, 85–90 (2000).
9. B. Chang, Y. Chen, Y. Zhao, R. K. Bruick, JMJD6 is a histone arginine demethylase. *Science* **318**, 444–447 (2007).
10. C. Poulard, J. Rambaud, N. Hussein, L. Corbo, M. Le Romancer, JMJD6 regulates ERα methylation on arginine. *PLoS One* **9**, e87982 (2014).
11. T.-F. Wu *et al.*, Loading of PAX3 to mitotic chromosomes is mediated by arginine methylation and associated with Waardenburg syndrome. *J. Biol. Chem.* **290**, 20556–20564 (2015).
12. P. Lawrence, J. S. Conderino, E. Rieder, Redistribution of demethylated RNA helicase A during foot-and-mouth disease virus infection: Role of Jumonji C-domain containing protein 6 in RHA demethylation. *Virology* **452-453**, 1–11 (2014).
13. M. Ganesan *et al.*, Demethylase JMJD6 as a new regulator of interferon signaling: Effects of HCV and ethanol metabolism. *Cell. Mol. Gastroenterol. Hepatol.* **5**, 101–112 (2017).
14. I. Tikhanovich *et al.*, Dynamic arginine methylation of tumor necrosis factor (TNF) receptor-associated factor 6 regulates Toll-like receptor signaling. *J. Biol. Chem.* **290**, 22236–22249 (2015).
15. W. W. Gao *et al.*, Arginine methylation of HSP70 regulates retinoid acid-mediated RARβ2 gene activation. *Proc. Natl. Acad. Sci. U.S.A.* **112**, E3327–E3336 (2015).
16. L. Wang, M. Wen, X. Cao, Nuclear hnRNPA2B1 initiates and amplifies the innate immune response to DNA viruses. *Science* **365**, eaav0758 (2019).
17. W. Liu *et al.*, Brd4 and JMJD6-associated anti-pause enhancers in regulation of transcriptional pause release. *Cell* **155**, 1581–1595 (2013).
18. J. Yang *et al.*, Jumonji domain-containing protein 6 protein and its role in cancer. *Cell Prolif.* **53**, e12747 (2020).
19. T. E. Miller *et al.*, Transcription elongation factors represent in vivo cancer dependencies in glioblastoma. *Nature* **547**, 355–359 (2017).
20. J. Yi *et al.*, JMJD6 and U2AF65 co-regulate alternative splicing in both JMJD6 enzymatic activity dependent and independent manner. *Nucleic Acids Res.* **45**, 3503–3518 (2017).
21. W.-W. Gao *et al.*, JMJD6 licenses ERα-dependent enhancer and coding gene activation by modulating the recruitment of the CARM1/MED12 co-activator complex. *Mol. Cell* **70**, 340–357.e8 (2018).
22. Y. F. Lee *et al.*, JMJD6 is a driver of cellular proliferation and motility and a marker of poor prognosis in breast cancer. *Breast Cancer Res.* **14**, R85 (2012).
23. J. Wan *et al.*, JMJD6 promotes hepatocellular carcinoma carcinogenesis by targeting CDK4. *Int. J. Cancer* **144**, 2489–2500 (2019).
24. C. R. Lee *et al.*, Elevated expression of JMJD6 is associated with oral carcinogenesis and maintains cancer stemness properties. *Carcinogenesis* **37**, 119–128 (2016).
25. X. Zhang *et al.*, JmjC domain-containing protein 6 (Jmjd6) derepresses the transcriptional repressor transcription factor 7-like 1 (Tcf7l1) and is required for body axis patterning during xenopus embryogenesis. *J. Biol. Chem.* **290**, 20273–20283 (2015).
26. T. Ran *et al.*, In silico discovery of JMJD6 inhibitors for cancer treatment. *ACS Med. Chem. Lett.* **10**, 1609–1613 (2019).
27. X. Hong *et al.*, Interaction of JMJD6 with single-stranded RNA. *Proc. Natl. Acad. Sci. U.S.A.* **107**, 14568–14572 (2010).
28. S. Lee *et al.*, JMJD6 cleaves MePCE to release positive transcription elongation factor b (P-TEFb) in higher eukaryotes. *eLife* **9**, e53930 (2020).
29. O. Aprelikova *et al.*, The epigenetic modifier JMJD6 is amplified in mammary tumors and cooperates with c-Myc to enhance cellular transformation, tumor progression, and metastasis. *Clin. Epigenetics* **8**, 38 (2016).
30. A. Biswas, G. Mukherjee, P. Kondaiah, K. V. Desai, Both EZH2 and JMJD6 regulate cell cycle genes in breast cancer. *BMC Cancer* **20**, 1159 (2020).
31. M. Wong *et al.*, JMJD6 is a tumorigenic factor and therapeutic target in neuroblastoma. *Nat. Commun.* **10**, 3319 (2019).
32. F. Wang *et al.*, JMJD6 promotes colon carcinogenesis through negative regulation of p53 by hydroxylation. *PLoS Biol.* **12**, e1001819 (2014).
33. A. Paschalis *et al.*; SU2C/PCF International Prostate Cancer Dream Team, JMJD6 is a druggable oxygenase that regulates AR-V7 expression in prostate cancer. *Cancer Res.* **81**, 1087–1100 (2021).
34. C. Zhang *et al.*, Epigenome screening highlights that JMJD6 confers an epigenetic vulnerability and mediates sunitinib sensitivity in renal cell carcinoma. *Clin. Transl. Med.* **11**, e328 (2021).
35. C. J. Webby *et al.*, Jmjd6 catalyses lysyl-hydroxylation of U2AF65, a protein associated with RNA splicing. *Science* **325**, 90–93 (2009).
36. J. E. Delmore *et al.*, BET bromodomain inhibition as a therapeutic strategy to target c-Myc. *Cell* **146**, 904–917 (2011).
37. Y. Liu *et al.*, JMJD6 regulates histone H2A.X phosphorylation and promotes autophagy in triple-negative breast cancer cells via a novel tyrosine kinase activity. *Oncogene* **38**, 980–997 (2019).
38. W. Liu et al., A specific JMJD6 inhibitor potently suppresses multiple types of cancers both in vitro and in vivo. NCBI's Gene Expression Omnibus. https://www.ncbi.nlm.nih.gov/geo/query/acc.cgi?acc=GSE201988. Deposited 2 May 2022.